Epitaxially grown $LiNbO_3$ thin films by polymeric precursor method

V. Bouquet,[a] M.I.B. Bernardi, S.M. Zanetti, E.R. Leite, and E. Longo
Departamento de Química—LIEC, Universidade Federal de São Carlos, P.O. Box 676, 13 565-905 São Carlos, SP, Brazil

J.A. Varela
Instituto de Química, Universidade Estadual Paulista, P.O. Box 355, 14884-970 Araraquara, SP, Brazil

M. Guilloux Viry and A. Perrin
Laboratoire Chimie du Solide et Inorganique Moléculaire, UMR CNRS 6511, Université de Rennes 1, Av. du Général Leclerc, 35 042 Rennes cedex, France

(Received 9 December 1999; accepted 9 August 2000)

$LiNbO_3$ thin films were grown on (0001) sapphire substrates by a chemical route, using the polymeric precursor method. The overall process consists of preparing a coating solution from the Pechini process, based on metallic citrate polymerization. The precursor films, deposited by dip coating, are then heat treated to eliminate the organic material and to synthesize the phase. In this work, we studied the influence of the heat treatment on the structural and optical properties of single-layered films. Two routes were also investigated to increase the film thickness: increasing the viscosity of the coating solution and/or increasing the number of successively deposited layers. The x-ray diffraction θ-2θ scans revealed the *c*-axis orientation of the single- and multilayered films and showed that efficient crystallization can be obtained at temperatures as low as 400 °C. The phi-scan diffraction evidenced the epitaxial growth with two in-plane variants. A microstructural study revealed that the films were crack free, homogeneous, and relatively dense. Finally, the investigation of the optical properties (optical transmittance and refractive index) confirmed the good quality of the films. These results indicate that the polymeric precursor method is a promising process to develop lithium niobate waveguides.

I. INTRODUCTION

In addition to its excellent ferroelectric and piezoelectric properties, lithium niobate ($LiNbO_3$ or LN) has large electro-optic and nonlinear optical coefficients.[1] These characteristics make LN an attractive material for optoelectronic and acousto-optical applications such as waveguides, modulators, second harmonic generators, and transducers.[2] For miniaturizing and integrating these devices, different processing methods have been developed to prepare LN thin films, including sol-gel process,[3–6] metalorganic decomposition (MOD),[7] chemical vapor deposition (CVD),[8] metalorganic chemical vapor deposition (MOCVD),[9] liquid phase epitaxy (LPE),[10] sputtering,[11,12] and pulsed laser deposition.[13–16] Compared to bulk devices, thin films are of much interest because they potentially allow monolithic integration with microelectronic or optoelectronic components. Moreover, microoptics such as channels and lenses can also be fabricated in thin films.[17,18]

For the above mentioned devices, the film must present well-defined features. In particular, the LN thin film should be epitaxially grown or at least highly textured since the properties of this anisotropic material depend on the crystallographic orientation. It is well known that the growth orientation strongly depends on the nature of the substrate. The use of silicon substrate for LN thin film deposition is interesting because it allows an integration compatible with the semiconductor technology, but usually only polycrystalline LN films are obtained.[19–22] However, some authors have succeeded in preparing textured LN thin films on silicon substrates, by sputtering or pulsed laser deposition, using a buffer layer[11] or an electric field during deposition.[13] Epitaxial LN thin films on $LiTaO_3$ and MgO-doped $LiNbO_3$ substrates have also been reported,[3] but the very small difference in optical index between the film and the substrate is not ideal for waveguide applications. The

[a]Address all correspondence to this author.
e-mail: p-bouquet@iris.ufscar.br

most common substrate used to obtain LN epitaxial thin films is sapphire. Despite the fact that sapphire has a large lattice mismatch and a thermal expansion coefficient significantly different from LN (Table I), it has the same structure and a much lower optical index. In addition to the required epitaxial or textured growth, the film must also present a minimal thickness estimated at 200–300 nm[23] and should be free of imperfections such as porosity and surface roughness. To achieve optical losses lower than 1 dB/cm, an R_{RMS} roughness of the order of 1 nm is required.[5]

In previous works, we have reported the preparation of LN thin films by the polymeric precursor method.[21,22,24] The overall process, also used to prepare other oxide thin films such as $SrTiO_3$[25] and $SrBi_2Nb_2O_9$,[26] consists of preparing a coating solution by the Pechini process, based on metallic citrate polymerization.[27] The precursor film is deposited by dip or spin coating and then heat treated to eliminate the organic material and synthesize the desired phase. The polymeric precursor method is attractive because it allows high stoichiometric control as well as the possibility of working with aqueous solution. Moreover, it is a low-temperature process and a cost-effective method. With this process, we have already succeeded in preparing polycrystalline LN thin films on silicon substrates.[21,22] We have also reported a preliminary work on LN thin films deposited on (0001) sapphire substrates.[24] The structural and surface characterization indicated films had (0001) oriented growth and surface smoothness of $R_{RMS} < 2$ nm (approximately 40 nm thick). However, the x-ray diffraction rocking curves full width at half-maximum (FWHM) revealed significant mosaic characteristics of the films (FWHM > 1.2°), which may be a limiting factor for waveguide applications.

The aim of the present study was to improve the microstructure of the LN thin films prepared by the polymeric precursor method, as well as to determine, for the first time, their optical properties. Two routes were also investigated to increase the film thickness.

II. EXPERIMENTAL

A. Coating solution preparation

The preparation of the coating solution was based on the Pechini process and has been reported in detail previously.[22] Lithium and niobium citrate solutions were prepared separately and then mixed together. The subsequent addition of ethylene glycol and the heating of the mixture led to a polymeric precursor solution, the viscosity of which was then adjusted by adding a controlled amount of H_2O.

B. Thin film process

The LN thin films were deposited by dip coating on (0001) sapphire substrates and then heat treated under flowing oxygen. The (0001) substrate orientation was chosen to promote the *c*-axis orientation of LN films, which is preferred for a waveguide device due to the large electro-optic and nonlinear optical coefficients of LN along this direction. The different parameters used for the film preparation are summarized in Table II.

For single-layered films prepared from a coating solution of 10 cP viscosity (films F1 to F4), various heat treatments were examined. In the earlier work,[24] an increase of the heating rate from 1 to 5 °C min^{-1} appeared to improve the film quality, while a treatment at temperature higher than 550 °C led to grain growth and surface degradation. Taking into account these results, in the present study we treated the single-layered films, from 400 to 550 °C, with heating and cooling rates of 5 °C min^{-1}. Two-step heat treatment was also examined, with a preheating at 350 °C for 2 h followed by a fast heating rate of 20 °C min^{-1} to reach the crystallization stage. It should be noted that this rapid heating rate was achieved without cracks occurring in the film because the organic material had already been eliminated during the pretreatment. The final thickness of the single-layered films varied from 36 to 71 nm, according to the heat treatment (Table II).

Additionally, two routes were investigated to increase the film thickness (films F5 to F11): increasing the viscosity of the coating solution or/and increasing the number of successively deposited layers, hereafter referred as "multilayered films." In the earlier work,[24] only the route of multilayered films was investigated, using the process "layer after layer crystallization." In the present study, 2- and 4-layered films were prepared in the following way: each layer deposition was followed by the pretreatment at 350 °C. A crystallization treatment was performed only after all the layers were deposited. According to the viscosity of the coating solution and to the number of layers, the final thickness of these films

TABLE I. Physical properties of $LiNbO_3$ and sapphire.[19,23]

	Crystal structure	Lattice parameters (Å)	Refractive indices at $\lambda = 632.8$ nm	Thermal expansion coefficient (at 25 °C)
$LiNbO_3$	Hexagonal	$a_h = 5.148$	$n_o = 2.286$	$\alpha_{11} = 15 \times 10^{-6}$
		$c_h = 13.863$	$n_e = 2.202$	$\alpha_{33} = 7.5 \times 10^{-6}$
Sapphire	Hexagonal	$a_h = 4.758$	$n_o = 1.758$	$\alpha_{11} = 8.3 \times 10^{-6}$
		$c_h = 12.990$	$n_e = 1.76$	$\alpha_{33} = 9.0 \times 10^{-6}$

TABLE II. Processing conditions and final thickness (determined by ellipsometry) of LN thin films prepared by the polymeric precursor method.

Film	Coating solution viscosity (cP)	Pretreatment	Heat treatment	Number of layers	Final thickness (nm)
F1	10	⋯	550 °C, 1 h	1	71
F2	10	⋯	450 °C, 4 h	1	44
F3	10	⋯	400 °C, 8 h	1	52
F4	10	350 °C, 2 h	550 °C, 2 h	1	36
F5	8	⋯	550 °C, 2 h	1	54
F6	15	⋯	550 °C, 2 h	1	70
F7	20	⋯	550 °C, 2 h	1	79
F8	10	350 °C, 2 h	550 °C, 2 h	2	50
F9	20	350 °C, 2 h	550 °C, 2 h	2	98
F10	10	350 °C, 2 h	550 °C, 2 h	4	71
F11	20	350 °C, 2 h	550 °C, 2 h	4	121

ranged from 50 to 121 nm (Table II). The study of their structural and optical properties will allow us to determine the best route to fabricate thicker films.

C. Characterization techniques

The structural characteristics of the films were investigated by x-ray diffraction (XRD) on a standard powder diffractometer (Siemens D5000, Germany) using $Fe_{K\alpha}$ radiation ($\lambda = 1937$ Å) with a manganese filter. In addition to the usual θ-2θ scans, the rocking curves (i.e., ω-scans) around the (0006) LN peak were recorded to measure the angular dispersion around the growth axis and thus to determine the orientation quality. The FWHM values of the rocking curves were determined by fitting the experimental curve with a Gaussian function. To study the in-plane orientation of the films, phi-scans were carried out with a texture diffractometer (Philips PW 3020, Holland).

The film surface morphology was observed with a field-emission scanning electron microscope (JEOL, JSM-6301F, Tokyo, Japan) operating at 7kV. The optical transmittance measurements were carried out in the wavelength range of 190–800 nm using a Cary 5G (Australia) spectrophotometer, and the refractive index was determined with an ellipsometer (Jobin Yvon, França) using a He–Ne laser beam ($\lambda = 632.8$ nm) with an incidence angle of 70° with respect to the normal of the sample.

III. RESULTS AND DISCUSSION

A. Structural characteristics

Figure 1(a) shows the θ-2θ scans, ranging from 5° to 55°, obtained for a single-layered film and a sapphire substrate. The only peak characteristic of LN that can be observed is the (0006) reflection, indicating high *c*-axis orientation of the film. All the other peaks were ascribed to the substrate. The θ-2θ scans obtained in the same range for all the single-layered films (F1 to F7) presented the same profile, revealed the *c*-axis-oriented growth, even for the films prepared from coating solutions of higher viscosity. For example, Figure 1(b) shows the XRD spectra restricted to the 45° to 55° range obtained for the films treated at different temperatures. The results revealed that crystallized films could be obtained at temperatures as low as 400 °C, which showed the potential of the polymeric precursor method. Note that some XRD spectra did not present the substrate peaks, which was due only to the sample position on the sample holder.

In the θ-2θ scans of the multilayered films (F8 to F11), the only peak characteristic of LN observed was also the (0006) reflection, indicating *c*-axis orientation. However, another peak was detected just beside the (0006) LN reflection. As an example, Figure 1(c) shows the XRD spectra restricted to the 45° to 55° range obtained for the multilayered films prepared using a 20 cP viscosity solution. The additional peak could not be indexed as a LN reflection and, thus, may have been due to another phase. It should be pointed out that this peak was not observed in the earlier work[24] for the multilayered films treated by the layer after layer crystallization process. Moreover, it was clearly observed that the relative intensity of this peak, compared to the (0006) LN line, strongly increased with the number of layers. A similar peak was already observed for LN thin films grown on sapphire substrate by pulsed laser deposition and was ascribed, in that case, to the $(\bar{6}02)$ $LiNb_3O_8$ reflection.[16,28] The authors succeeded in eliminating this Li-depleted phase, which is undesirable because it is not ferroelectric, by using Li-enriched targets[28] or increasing the oxygen flow during deposition.[16] The preferred orientation of $LiNb_3O_8$ on *c*-cut sapphire is attributed to the small difference in the ionic arrangements of the $(\bar{6}02)$ $LiNb_3O_8$ plane and the (006) sapphire plane, as explained by Fujirama *et al.*[29] In this present study, further investigations are in progress to confirm the presence of the $LiNb_3O_8$ phase and to localize it, i.e., to determine if it forms at the film–

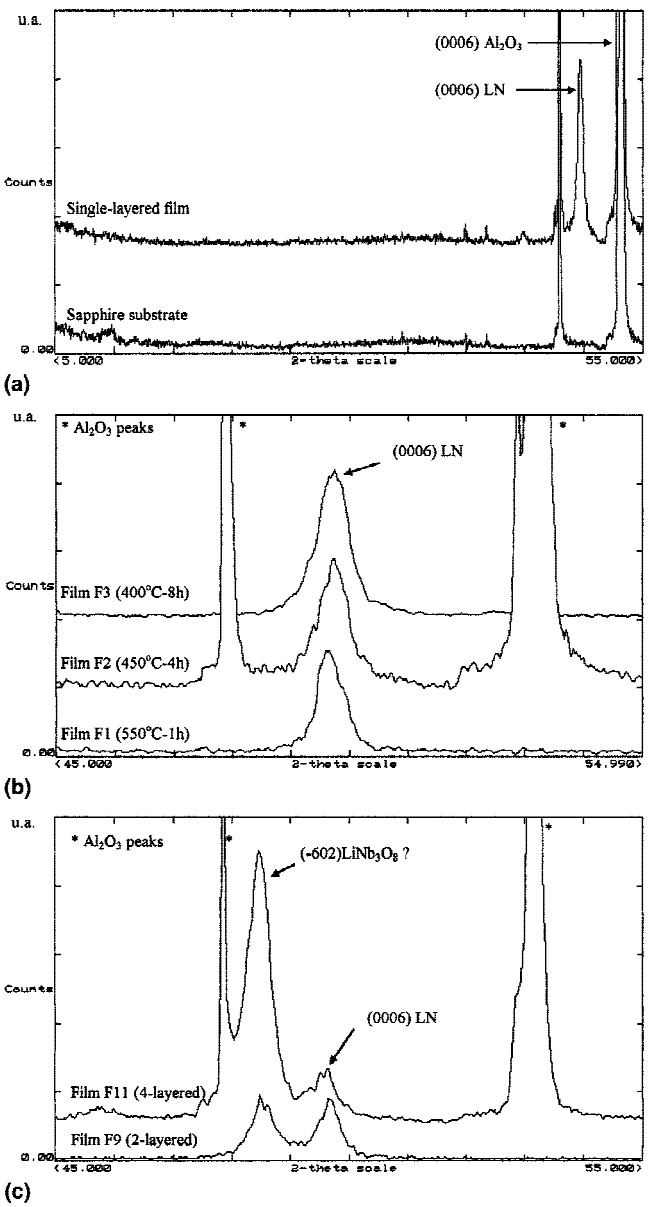

FIG. 1. (a) XRD patterns for a single-layered film and a sapphire substrate. (b) XRD patterns of single-layered films prepared from a 10-cP viscosity solution and heat treated at different temperatures. (c) XRD patterns of multilayered films prepared from a 20-cP viscosity solution and heat treated under the same conditions.

substrate interface, as a result of a possible difficulty for the oxygen flow to reach this region. We supposed a vertical distribution rather than a lateral distribution because the peak was not observed for single-layered films. The present results suggested that the presence of this peak was directly connected to the heat-treatment process of the multilayered films used in this work.

The (0006) LN rocking curves obtained for the single and multilayered films presented similar profiles, illustrated in Fig. 2(a). A very narrow peak with FWHM as low as 0.08°, revealing the high degree of orientation, was observed. This value, in agreement with FWHM reported in literature,[6,9] was very good, considering the large lattice and thermal expansion mismatch between the film and substrate. Note that this value could be considered as the instrumental broadening of the diffractometer since the FWHM value obtained for the (0006) sapphire substrate was almost identical: 0.07° [Figure 2(b)]. However, the rocking curves of the films presented a relatively broad tail with FWHM varying from 1.46° to 2.81°, according to the processing parameters. The presence of a broad tail had already been observed by some authors for the same film/substrate couple[6] and also for other systems such as CeO_2/sapphire.[30] A profile such as this one indicates the coexistence of a nearly perfect material and a little more distorted one. In the case of CeO_2 grown on sapphire by pulsed laser deposition, X. Castel *et al.*[30] suggested that the top surface had a very good crystallographic structure whereas the interface with the substrate was distorted. Furthermore, H. Nashimoto *et al.*[6] also proposed a "two-layer" structure in the case of LN thin films prepared by sol-gel, but considering the highly oriented layer near the film–substrate interface. In our case, it is difficult to conclude the nature of the structure without performing other experiments. However, the large lattice mismatch between the film and the substrate could create disorder at the interface, which might lead to the presence of a distorted region at the interface.

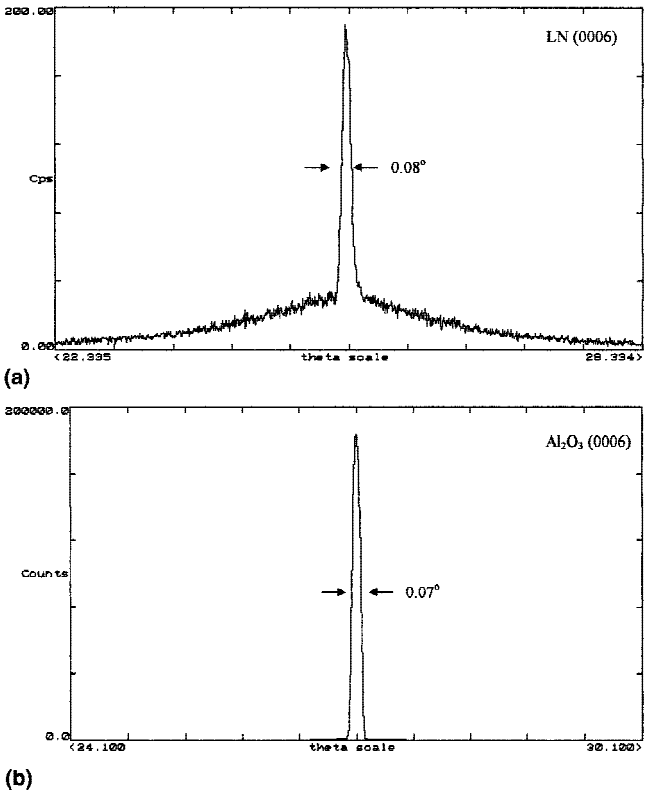

FIG. 2. Rocking curves (a) around the (0006) LN peak and (b) around the (0006) sapphire substrate peak.

Figures 3(a), 3(b), and 3(c) illustrate the phi-scan of the LN ($20\bar{4}$) peak obtained for the single- and multilayered films prepared using a 10-cP viscosity solution and heat treated under the same conditions (films F4, F8, and F10). Because LN has a 3*m* crystal symmetry (space group *R*3*c*), a single crystal (or a quasi-single crystal such as an epitaxial film) should present a threefold symmetry in the phi-scan. In Fig. 3(a), a set of three main peaks, spaced by 120°, revealed the epitaxial growth of the single-layered film. However, an additional set of three peaks with lower intensity was observed, also presenting a threefold symmetry and separated by 60° from the main peaks. This result suggested the presence in the epitaxial film of two variants rotated by 60° (or, equivalently 180°) with respect to each other about the *c*-axis.

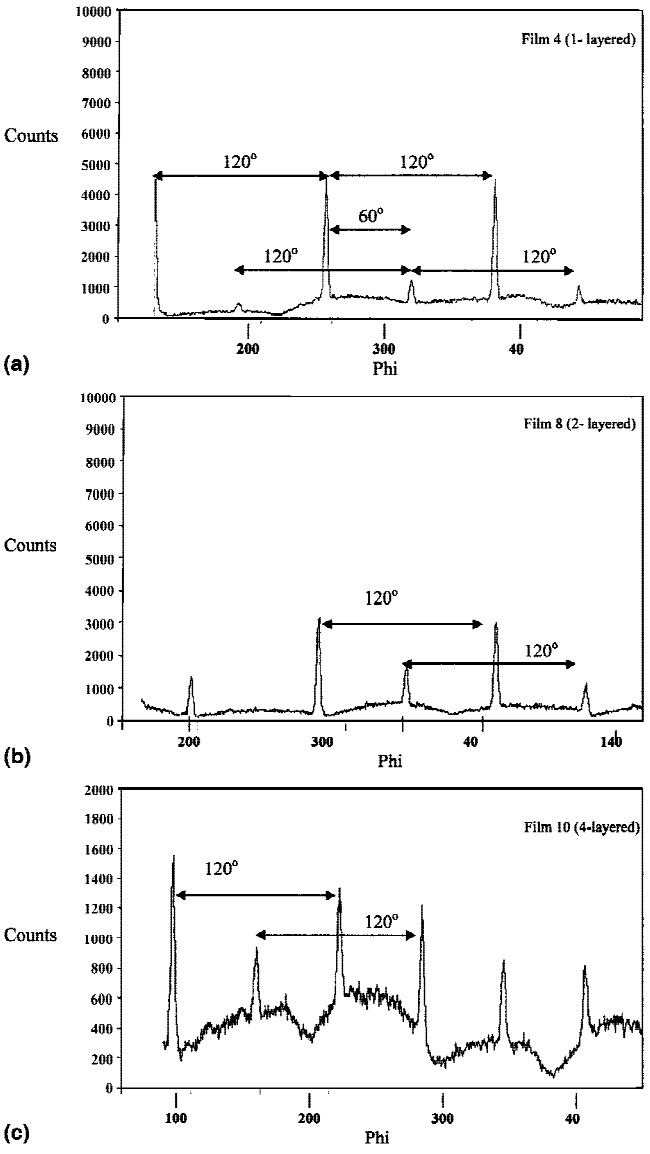

FIG. 3. X-ray phi-scans of films prepared from a 10-cP viscosity solution and heat treated under the same conditions: (a) single-layered film F4, (b) 2-layered film F8, and (c) 4-layered film F10.

The phi-scans of the multilayered films were also composed of two sets of three peaks, but it appeared clearly that the relative intensity of these two groups depended on the number of layers [Figures 3(b) and 3(c)]. The volume fraction of the 60° rotated grains, calculated from the integrated intensity, represented 7% of the total diffracted volume for the single-layered film. This volume increased to 21% for the 2-layered film and reached 42% for the 4-layered film. It should be pointed out that this increase was not observed for multilayered films treated by the layer after layer crystallization process.

The presence of two in-plane variants in LN epitaxial thin films has already been observed and discussed by several authors.[5,31] According to Derouin *et al.*,[5] the cation positions, and not the oxygen packing, are responsible for the two orientations observed in LN thin films prepared by sol-gel. The authors suggested that the presence of the 60° variant was partially strain driven and, therefore, was influenced by lattice mismatch between the film and substrate and also by the film thickness. Strain in the film is minimized by the creation of dislocations, which leads to cation disorder. Feigelson[31] also observed the two variants in LN thin films prepared by MOCVD and explained that rotated grains were not energetically favorable and could be eliminated by postannealing. In the present work, the fact that crystallization treatment was performed only after all the layers had been deposited led to an increase of strains and, therefore, to an increase of the misalignment in the plane of the film.

B. Surface morphology

The microstructure study revealed that all the films were crack free and homogeneous. To observe the presence of pores, high-resolution SEM observation (100,000×) was performed. Figures 4(a), 4(b), and 4(c) display the micrographs obtained for the single- and multilayered films prepared from 10-cP viscosity solution and heat treated under the same conditions (films F4, F8 and F10). It was observed that the size, shape, and quantity of pores were modified with the increase of the layer number. Whereas the single-layered film presented some circular pores with an average 20-nm diameter, the 2-layered film had pores of irregular shape, more elongated (approximately 40-nm length and approximately 15-nm width). Some irregular pores were also present in the 4-layered film but were smaller. A similar microstructural evolution with the number of the deposited layers was also observed for the films prepared from the 20-cP viscosity solution. It should be pointed out that it is important to control the film porosity, particularly for optical applications. A highly densified film is expected to have a high refractive index close to the single crystal value.

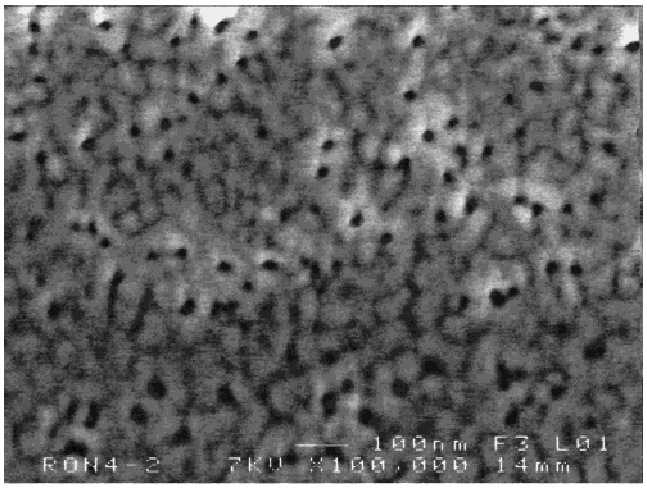

(a)

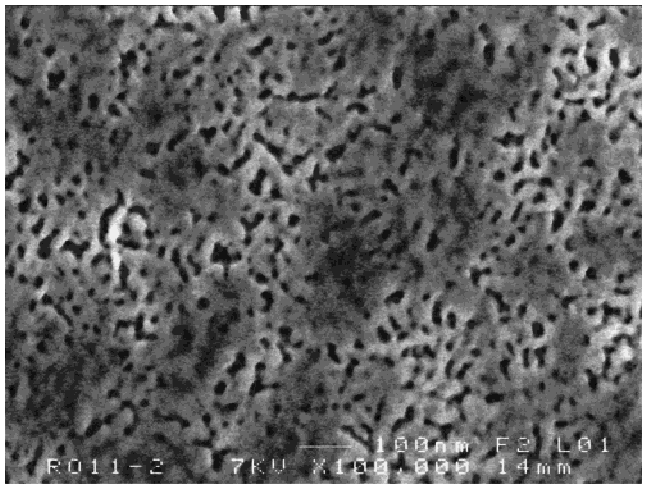

(b)

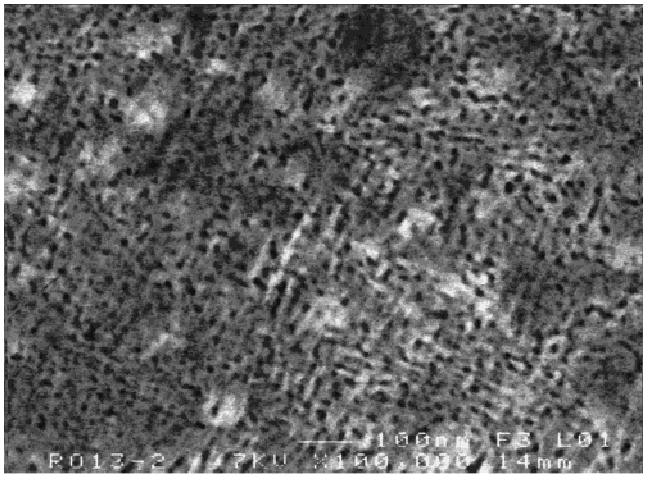

(c)

FIG. 4. SEM micrographs of films prepared from the 10-cP viscosity solution and heat treated under the same conditions: (a) single-layered film F4, (b) 2-layered film F8, and (c) 4-layered film F10.

C. Optical properties

Figure 5(a) shows the transmission spectra in the ultraviolet–visible region obtained for the sapphire substrate and the single-layered films prepared from the 10-cP viscosity solution and heat treated at different temperatures. From $\lambda = 250$ nm, the transmittance of the films began to increase and reached 65% at $\lambda = 350$ nm. Hur *et al.*[19] observed a drastic rise of the transmittance at a longer wavelength, about 300 nm, with LN films prepared by sol-gel. In the spectral region of 400–800 nm, the samples exhibited a high transmission (>70%), which confirmed that the films were relatively dense and homogeneous. Moreover, as the optical transmittance is strongly affected by composition,[4] these results suggested that the films were stoichiometric. On the other hand, the increase of the solution viscosity affected the shape of the cutoff, as shown in Figure 5(b). In particular, the film prepared from the 20-cP viscosity solution (film F7) presented a relatively steep transmittance cutoff, close to the single LN crystal behavior, and, therefore, it indicated an excellent otpical quality. The multi-

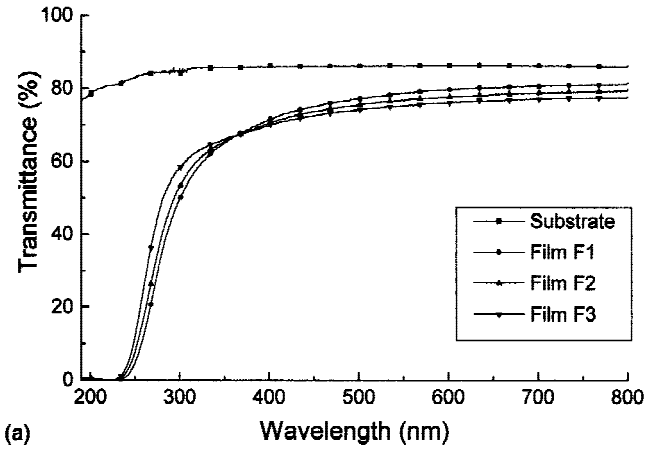

(a)

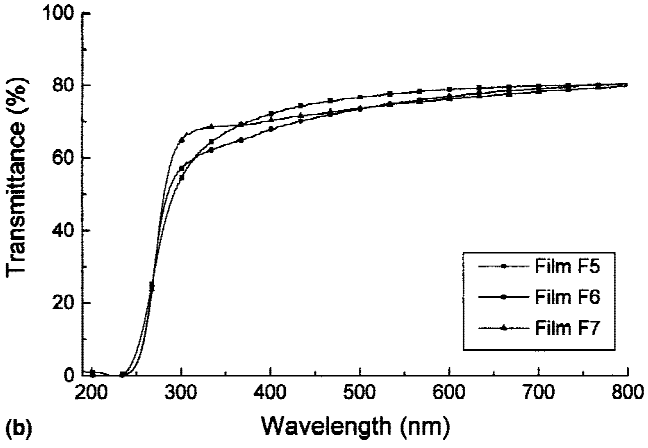

(b)

FIG. 5. (a) Ultraviolet–visible (UV-VIS) transmission spectra for a sapphire substrate and for single-layered films prepared from a 10-cP viscosity solution and heat treated at different temperatures. (b) UV-VIS transmission spectra for single-layered films prepared from coating solutions of different viscosities and heat treated at 550 °C for 2 h.

layered films also presented a high transmission (>70%) in the spectral region of 400–800 nm. However, a slight shift of the cutoff to longer wavelength for the 4-layered films (F9 and F11) was observed, which may have been due to the large increase in film thickness, as suggested by Zhu *et al.*[32]

Table III summarizes the refractive indices of the different films, calculated from the ellipsometric measurements. As lithium niobate presents anisotropic properties, the refractive index depends on the crystallographic orientation. For the LN bulk crystal, the refractive indices at $\lambda = 632.8$ nm are $n_e = 2.202$ (extraordinary index) and $n_o = 2.286$ (ordinary index), along the *c*-axis direction and in the direction normal to the *c*-axis, respectively.[1] However, the ellipsometric method does not allow the separation of these two indices. The single-layered films prepared from the 10-cP viscosity solution and heat treated at different temperatures (films F1 to F4) presented a refractive index varying from 2.035 to 2.24. These values were in agreement with those reported in literature for $LiNbO_3$.[6,16,33] Note that the refractive index is mainly influenced by the crystallinity and density of the film,[33] which explains its variation according to the heat treatment performed on the precursor film. In particular, the low index obtained for the film treated at 400 °C suggested the presence of amorphous or not well-crystallized regions in this sample. The higher refractive index, close to that of the LN bulk crystal, was obtained for the film prepared from the 20-cP viscosity solution (film F7), confirming the high optical quality already suggested by the transmittance curve (steep cutoff). The 2- and 4-layered films presented a refractive index ranging from 2.08 to 2.15. These results are promising, considering that the crystallinity and density of these multilayered films can probably be improved using the "layer after layer crystallization" process.

Considering all these results, a 10-layered film was successfully prepared from a 20-cP viscosity solution, using the layer after layer crystallization process. The film approximately 420 nm thick presented an epitaxial growth and a crack-free, homogeneous and smooth surface[34] (Fig. 6). The R_{RMS} value, obtained for an area of 1×1 μm, was 2.5 nm. The investigation of the optical properties of this film (transmittance, refractive index, and optical loss) is currently in progress.

TABLE 3. Refractive index of LN thin films, determined by ellipsometry.

Film	Refractive index
F1	2.11
F2	2.24
F3	2.03
F4	2.08
F5	2.05
F6	2.14
F7	2.27
F8	2.09
F9	2.12
F10	2.15
F11	2.08

IV. CONCLUSION

C-axis-oriented LN thin films were grown on *c*-cut sapphire by polymeric precursor method, at treatment temperatures as low as 400 °C. The shape of the rocking curves suggested a two-layer structure formed by a nearly perfect material (FWHM = 0.08°) and a little more distorted one (presence of a broad tail). The increase of the coating solution viscosity and the successive deposition of several layers enabled us to increase in the film thickness without affecting significantly the *c*-axis orientation and without inducing cracks in the film. The in-plane diffraction measurement revealed the epitaxial growth of the films, with two in-plane variants. The volume fraction of the 60° rotated grains increased with the number of layers, probably due to the fact that crystallization treatment was performed only after all the layers had been deposited, which led to an increase of strain.

In addition to their homogeneous and relatively dense microstructure, the films exhibited promising optical properties. In particular, the single-layered film prepared from the higher viscosity solution (20 cP) presented a transmittance spectrum and a refractive index close to those of a LN bulk crystal. In the case of the 2- and 4-layered films, the results suggested that to perform the crystallization treatment only after all the layers had been deposited was not ideal. Therefore, the layer after layer

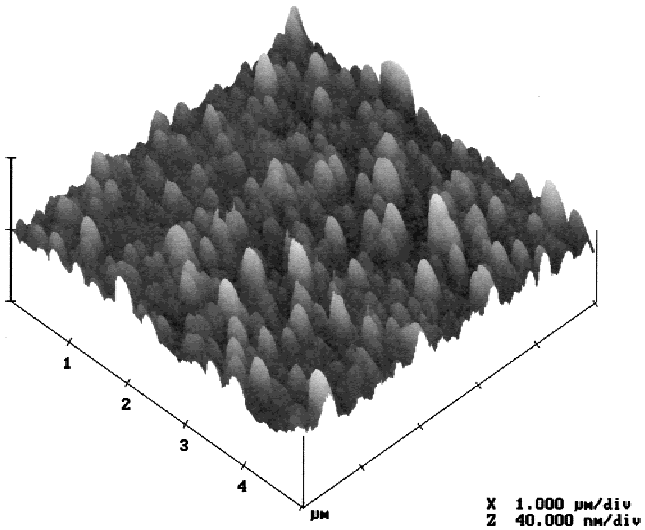

FIG. 6. Atomic force microscope image of a 10-layered film prepared from a 20-cP viscosity solution.

crystallization process was used to prepare a 10-layered film from a 20 cP viscosity solution. The preliminary results obtained with this 420-nm-thick film showed that the polymeric precursor method is promising to prepare LN waveguides.

ACKNOWLEDGMENTS

The authors acknowledge the CAPES/COFECUB and the FAPESP for the financial support. Electron microscope data were collected at CMEBA, Center for Electron Microsopy and Microanalysis of University of Rennes 1. The ellipsometry measurements were carried out at CCMO of University of Rennes 1.

REFERENCES

1. R.S. Weis and T.K. Gaylord, Appl. Phys. **A37,** 191 (1985).
2. M.M. Abouelleil and F.G. Leonberger, J. Am. Ceram. Soc. **72,** 1311 (1989).
3. K. Terabe, N. Iyi, K. Kitamura, and S. Kimura, J. Mater. Res. **10,** 1779 (1995).
4. S. Ono and S. Hirano, J. Am. Ceram. Soc. **80,** 2533 (1997).
5. T.A. Derouin, C.D.E. Lakeman, X.H. Wu, J.S. Speck, and F.F. Lange, J. Mater. Res. **12,** 1391 (1997).
6. K. Nashimoto, H. Moriyama, and E. Osakabe, Jpn. J. Appl. Phys., Part 1 **35,** 4936 (1996).
7. G. Braunstein, G.R. Paz-Pujalt, and T.N. Blanton, Thin Solid Films **264,** 4 (1995).
8. N. Yamaguchi, T. Hattori, K. Terashima, and T. Yoshida, Thin Solid Films **316,** 185 (1998).
9. S.Y. Lee and R.S. Feigelson, J. Cryst. Growth **186,** 594 (1998).
10. K. Kaigawa, T. Kawaguchi, M. Imaeda, H. Sakai, and T. Fukuda, J. Cryst. Growth **177,** 217 (1997).
11. S. Tan, T. Gilbert, C-Y. Hung, T.E. Schlesinger, and M. Migliuolo, J. Appl. Phys. **79,** 3548 (1996).
12. T. Nishida, K. Ishida, T. Horiuchi, T. Shiosaki, and K. Matsushige, Jpn. J. Appl. Phys., Part 2 **35,** L1699 (1996).
13. Z.G. Liu, W.S. Hu, X.L. Guo, J.M. Liu, and D. Feng, Appl. Surf. Sci. **109/110,** 520 (1997).
14. J. Gonzalo, C.N. Afonso, J.M. Ballesteros, A. Grosman, and C. Ortega, J. Appl. Phys. **82,** 3129 (1997).
15. S.H. Lee, T.W. Noh, and J.H. Lee, Appl. Phys. Lett. **68,** 472 (1996).
16. P. Aubert, G. Garry, R. Bisaro, and J. Garcia Lopez, Appl. Surf. Sci. **86,** 144 (1995).
17. K. Nashimoto, K. Haga, M. Watanabe, S. Nakamura, and E. Osakabe, Appl. Phys. Lett. **75,** 1054 (1999).
18. K. Nashimoto, S. Nakamura, T. Morikawa, H. Moriyama, M. Watanabe, and E. Osakabe, Appl. Phys. Lett. **74,** 2761 (1999).
19. N.H. Hur, Y.K. Park, D.H. Won, and K. No, J. Mater. Res. **9,** 980 (1994).
20. S.B. Ogale, R. Nawathey-Dikshit, S.J. Dikshit, and S.M. Kanetkar, J. Appl. Phys. **71,** 5718 (1992).
21. V. Bouquet, S.M. Zanetti, C.R. Foschini, E.R. Leite, E. Longo, and J.A. Varela, in *Innovative Processing and Synthesis of Ceramics, Glasses and Composites,* edited by N.P. Bansal, K.V. Logan, and J.P. Singh, (Ceram. Trans. **85,** Am. Ceram. Soc., Westerville, OH, 1997), p. 333.
22. V. Bouquet, E. Longo, E.R. Leite, and J.A. Varela, J. Mater. Res. **14,** 3115 (1999).
23. S. Schwyn, H.W. Lehman and R. Widmer, J. Appl. Phys. **72,** 1154 (1992).
24. V. Bouquet, E.R. Leite, E. Longo, and J.A. Varela, J. Eur. Ceram. Soc. **19,** 1447 (1999).
25. S.M. Zanetti, E.R. Leite, E. Longo, and J.A. Varela, Appl. Organometal. Chem. **13,** 373 (1999).
26. S.M. Zanetti, E.R. Leite, E. Longo, and J.A. Varela, J. Mater. Res. **14,** 1026 (1999).
27. M.P. Pechini, U.S. Patent No. 3. 330 697 (1967).
28. Y. Shibata, K. Kaya, K. Akashi, M. Kanai, T. Kawai, and S. Kawai, J. Appl. Phys. **77,** 1498 (1995).
29. N. Fujimura and T. Ito, J. Cryst. Growth **115,** 821 (1991).
30. X. Castel, M. Guilloux-Viry, A. Perrin, J. Lesueur, and F. Lalu, J. Cryst. Growth **187,** 211 (1998).
31. R.S. Feigelson, J. Cryst. Growth **166,** 1 (1996).
32. J.S. Zhu, X.M. Lu, W. Jiang, W. Tian, M. Zhu, M.S. Zhang, X.B. Chen, X. Liu, and Y.N. Wang, J. Appl. Phys. **81,** 1392 (1997).
33. S. Ono, O. Bose, W. Unger, Y. Takeichi, and S. Hirano, J. Am. Ceram. Soc. **81,** 1749 (1998).
34. V. Bouquet, Internal report, LiEC-DQ, UFSCar, Saõ Carlos, SP, Brazil (2000).